



The Design and Testing of a High-Temperature Graphite Dilatometer

Prepared by

P. M. SHEAFFER and G. W. HENDERSON
Mechanics and Materials Technology Center
Technology Operations

24 June 1992

Prepared for

SPACE SYSTEMS DIVISION
AIR FORCE SYSTEMS COMMAND
Los Angeles Air Force Base
P. O. Box 92960
Los Angeles, CA 90009-2960

SDTIC
ELECTE
MAR 18 1993
E D

Engineering and Technology Group

93-05471



THE AEROSPACE CORPORATION

El Segundo, California



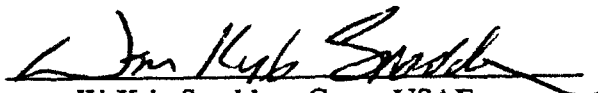
APPROVED FOR PUBLIC RELEASE;
DISTRIBUTION UNLIMITED

98 3 16 092

This report was submitted by The Aerospace Corporation, El Segundo, CA 90245-4691, under Contract No. F04701-85-C-0086-P00019 with the Space Systems Division, P. O. Box 92960, Los Angeles, CA 90009-2960. It was reviewed and approved for The Aerospace Corporation by R. W. Fillers, Principal Director, Mechanics and Materials Technology Center. P. M. Propp was the project officer for the Mission-Oriented Investigation and Experimentation (MOIE) program.

This report has been reviewed by the Public Affairs Office (PAS) and is releasable to the National Technical Information Service (NTIS). At NTIS, it will be available to the general public, including foreign nationals.

This technical report has been reviewed and is approved for publication. Publication of this report does not constitute Air Force approval of the report's findings or conclusions. It is published only for the exchange and stimulation of ideas.



W. Kyle Sneddon, Capt., USAF
MOIE Program Manager



Paul M. Propp
Wright Laboratory
West Coast Office

UNCLASSIFIED

SECURITY CLASSIFICATION OF THIS PAGE

REPORT DOCUMENTATION PAGE

1a. REPORT SECURITY CLASSIFICATION Unclassified			1b. RESTRICTIVE MARKINGS			
2a. SECURITY CLASSIFICATION AUTHORITY			3. DISTRIBUTION/AVAILABILITY OF REPORT			
2b. DECLASSIFICATION/DOWNGRADING SCHEDULE			Approved for public release; distribution unlimited			
4. PERFORMING ORGANIZATION REPORT NUMBER(S) TR-0088(3935-06)-2			5. MONITORING ORGANIZATION REPORT NUMBER(S) SSD-TR-92-25			
6a. NAME OF PERFORMING ORGANIZATION The Aerospace Corporation Laboratory Operations		6b. OFFICE SYMBOL (if applicable)	7a. NAME OF MONITORING ORGANIZATION Space Systems Division			
6c. ADDRESS (City, State, and ZIP Code) El Segundo, CA 90245			7b. ADDRESS (City, State, and ZIP Code) Los Angeles Air Force Base Los Angeles, CA 90009-2960			
8a. NAME OF FUNDING/SPONSORING ORGANIZATION		8b. OFFICE SYMBOL (if applicable)	9. PROCUREMENT INSTRUMENT IDENTIFICATION NUMBER F04701-85-C-0086-P00019			
8c. ADDRESS (City, State, and ZIP Code)			10. SOURCE OF FUNDING NUMBERS			
			PROGRAM ELEMENT NO.	PROJECT NO.	TASK NO.	WORK UNIT ACCESSION NO.
11. TITLE (Include Security Classification) The Design and Testing of a High-Temperature Graphite Dilatometer						
12. PERSONAL AUTHOR(S) Sheaffer, Patrick M., and Henderson, George W.						
13a. TYPE OF REPORT		13b. TIME COVERED FROM _____ TO _____		14. DATE OF REPORT (Year, Month, Day) 1992 June 24		15. PAGE COUNT 51
16. SUPPLEMENTARY NOTATION						
17. COSATI CODES			18. SUBJECT TERMS (Continue on reverse if necessary and identify by block number)			
FIELD	GROUP	SUB-GROUP	Carbon	Dilatometry		
			Graphite	Thermal strain		
			Pyrolysis	Glassy carbon		
			Composites (carbon-carbon)	Thermal expansion		
19. ABSTRACT (Continue on reverse if necessary and identify by block number) A dilatometer for investigating the high-temperature behavior of carbonaceous materials has been constructed within a graphite tube furnace in the Composites Section of the Mechanics and Materials Technology Center of The Aerospace Corporation. The dilatometer is a single-pushrod type with a linear variable differential transformer (LVDT) dilation measurement system and employs computer data acquisition and analysis. It can measure thermally induced strain of a sample from room temperature to over 3000°C, a temperature that has been difficult to reach with currently available laboratory apparatus. The estimated uncertainty of the dilation measurement system is about ± 5 μm over the entire temperature range. All components in the hot zone, including the sample holder and pushrod, are made of polycrystalline graphite. A three-point-bend fixture can be placed in the apparatus to measure the rheological properties of a pyrolyzing carbon precursor or the high-temperature creep properties of a carbon under conditions of constant flexural stress.						
20. DISTRIBUTION/AVAILABILITY OF ABSTRACT <input type="checkbox"/> UNCLASSIFIED/UNLIMITED <input checked="" type="checkbox"/> SAME AS RPT. <input type="checkbox"/> DTIC USERS				21. ABSTRACT SECURITY CLASSIFICATION Unclassified		
22a. NAME OF RESPONSIBLE INDIVIDUAL			22b. TELEPHONE (Include Area Code)		22c. OFFICE SYMBOL	

CONTENTS

I. INTRODUCTION..... 5

II. DESCRIPTION OF APPARATUS AND SAFETY CONSIDERATIONS..... 7

III. CALIBRATION OF THE INSTRUMENT..... 13

A. THEORETICAL..... 13

B. PRACTICAL ASPECTS OF DILATOMETER CALIBRATION..... 17

IV. RESULTS..... 23

V. CONCLUSIONS..... 29

REFERENCES..... 31

APPENDIX A. DILATOMETER DATA ACQUISITION PROGRAM..... 33

APPENDIX B. DILATOMETER DATA ANALYSIS PROGRAM..... 39

Accession For	
NTIS CRA&I	<input checked="" type="checkbox"/>
DTIC TAB	<input type="checkbox"/>
Unannounced	<input type="checkbox"/>
Justification	
By	
Distribution /	
Availability Codes	
Dist	Avail and/or Special
A-1	

FIGURES

1.	Cutaway view of the dilatometer, showing LVDT and sample tube/pushrod assembly in place.....	8
2.	Heat flow out of furnace case as measured from change in the temperature of the cooling water flowing at a known rate, $\dot{Q} = mc \Delta T$, and approximate times for the exterior of the furnace to reach melting temperature.....	9
3.	Diagram of the cooling-tower water system for the dilatometer furnace.....	11
4.	Schematic of a single-pushrod dilatometer.....	14
5.	Thermal strain data from optical calibration of the in-house-developed pyrolytic graphite standard, published data for ATJ-S polycrystalline graphite, and theoretical basal-plane expansion of graphite.....	18
6.	(a) Initial dilatometer measurement, following calibration, on NIST sapphire standard reference material SRM 738 (solid line). The published data for this material are displayed pointwise as open circles. The deviation between measured and published data is also shown (dashed line). The indicated error is in the optical calibration data ($> 700^\circ\text{C}$). (b) Two successive runs on SRM 738 after subtracting deviation data (extrapolated to 3000°C) from graphite-standard calibration curve. (See also Fig. 5.) Published data for SRM 738 are also shown, as open circles.....	20
7.	Thermal expansion data for ATJ-S polycrystalline graphite samples of different lengths.....	21
8.	Uncorrected thermal strain data from pyrolytic graphite.....	24
9.	True thermal strain response of pyrolytic graphite in basal-plane-normal direction for the second run, and parallel to the basal plane for the first and second runs, respectively.....	25
10.	Thermal strain of several carbon-carbon composite configurations.....	26
11.	Data from three-point-bend samples of PAA, phenolic, and furfural resin samples that were precured to 350°C	28

I. INTRODUCTION

Carbon-carbon (C-C) composites have established themselves as important high-temperature materials for spacecraft applications. Proposed new aerospace designs such as those in the National Aerospace Plane (NASP) and in advanced turbine engines also utilize C-C composites extensively.

Some C-C composites are graphitic materials. Such materials, including carbon-fiber-reinforced carbon-matrix composites, are generally manufactured at temperatures exceeding 2400°C. Glassy-carbon-matrix C-C composites also are frequently heat-treated to relatively high temperatures, above 1700°C, to achieve their maximum mechanical properties.¹ When such advanced composite materials are used for applications requiring high thermal stability, thermal strain becomes an important engineering property.

The bulk thermal strain of C-C composites is ideally described in terms of the properties of the constituent materials. Improved composites can then be designed without the laborious trial-and-error of manufacturing test composites. However, C-C composites are complex, and this type of predictive design is difficult to apply. Thermal strain, the reversible dimensional change associated with heating, is an approximately linear expansion for most solids² but not for graphite. Graphite's basal plane has a minimum strain near 400°C, and there is a large crystallographic thermal expansion anisotropy between the basal plane and the c-axis. These factors make precise thermoelastic modeling of a composite difficult. Also, data are lacking on the pyrolysis and high-temperature behavior of precursors and matrix carbons. During the manufacture of a C-C composite, the carbon matrix precursor is pyrolyzed and carbonized to convert it to carbon or graphite. In the process, the matrix densifies and a complex crack network and stress field form in the matrix and at the matrix-filament interfaces,³ making it difficult to form an a priori estimate of the final thermal strain of a given composite design. Further investigation of the matrix pyrolysis behavior and its correlation with bulk thermal strain is therefore required.

A problem arises in laboratory investigations of such phenomena over the 2000-to-3000°C range: The upper temperature limit of most commercially available high-temperature dilatometers is only about 2000°C. We therefore constructed and tested a high-temperature graphite dilatometer that can accurately measure thermal strain phenomena at temperatures as high as 3000°C. Before this apparatus was constructed, high-temperature dilatometric and rheological measurements could not be carried out at The Aerospace Corporation, and such facilities are generally not available at commercial testing laboratories.

This report describes the dilatometer and is organized as follows. The primary components of the dilatometer system are described in Section II. The theoretical and practical aspects of dilatometer calibration and the method of data reduction are discussed in Section III. Finally, initial experiments to measure thermal strain on several carbonaceous materials with the dilatometer are summarized in Section IV.

II. DESCRIPTION OF APPARATUS AND SAFETY CONSIDERATIONS

The dilatometer, diagrammed in Fig. 1, consists of a sample tube/pushrod and a cage assembly that are fabricated from a single billet of polycrystalline graphite to ensure uniformity of thermal expansion. The sample cage can be removed from the sample tube so that other cages can be fabricated and installed to accommodate samples of different sizes. The sample pushrod extends coaxially through the sample tube to make contact with the sample. The mass of the pushrod (~10 g) serves to keep it in contact with the sample during the test. A linear variable differential transformer (LVDT), whose core is fixed to the pushrod, measures the displacement of the pushrod (as the sample expands upon heating) and sends an electrical signal to a data acquisition system. The heating elements, which are also made from graphite, are located coaxially around the sample cage.

The furnace (manufactured by Astro Division of Thermal Technologies Inc.) consists, from the heating elements outward, of a graphite retort around which is packed thermal insulation (lampblack and graphite felt), encased in an airtight, water-cooled aluminum housing. The interior of the aluminum housing is purged with an inert atmosphere during the test to prevent oxidation of the insulation and retort, heating elements, sample holder assembly, and sample. The furnace case and the LVDT are cooled by flowing water from the laboratory cooling-tower water supply.

The cooling water has an emergency city-water (tap water) backup. If the cooling-tower water flow is interrupted, e.g., by a power outage, two valves can be manually opened to provide city-water cooling to the furnace case. The cooling-tower water lines are monitored by a flow sensor that sounds an alarm (100-dB intensity) and shuts off the furnace power when the cooling-water flow rate drops below normal. Following such an interruption, the time allowed at a given temperature before the aluminum furnace housing fails from overheating has been estimated by heat flow calculations (see Fig. 2). At a maximum operating temperature of 2500°C, 5 min would be

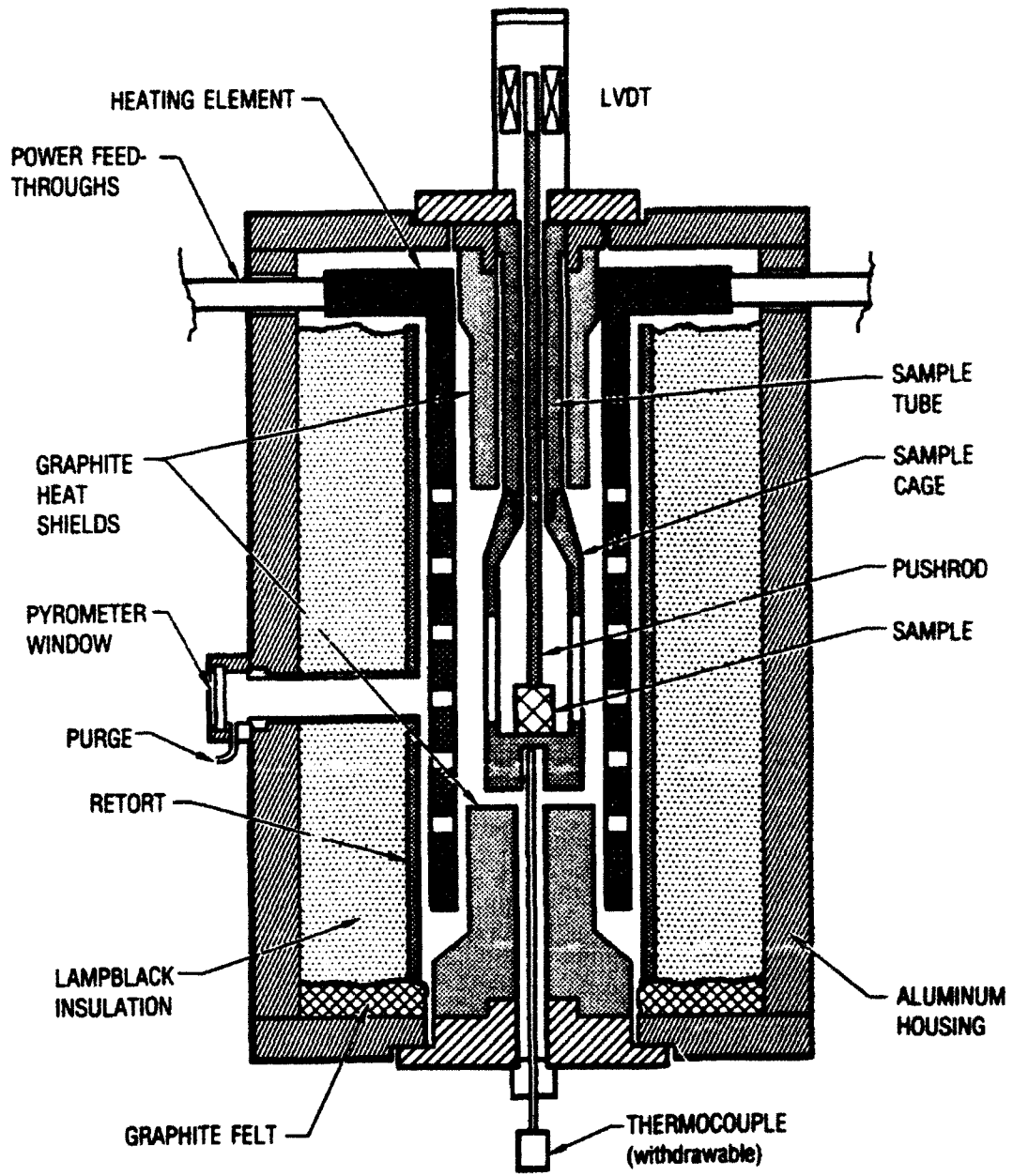


Fig. 1. Cutaway view of the dilatometer, showing LVDT and sample tube/pushrod assembly in place. The top closure of the furnace, which supports the LVDT, and the entire aluminum furnace case are water-cooled.

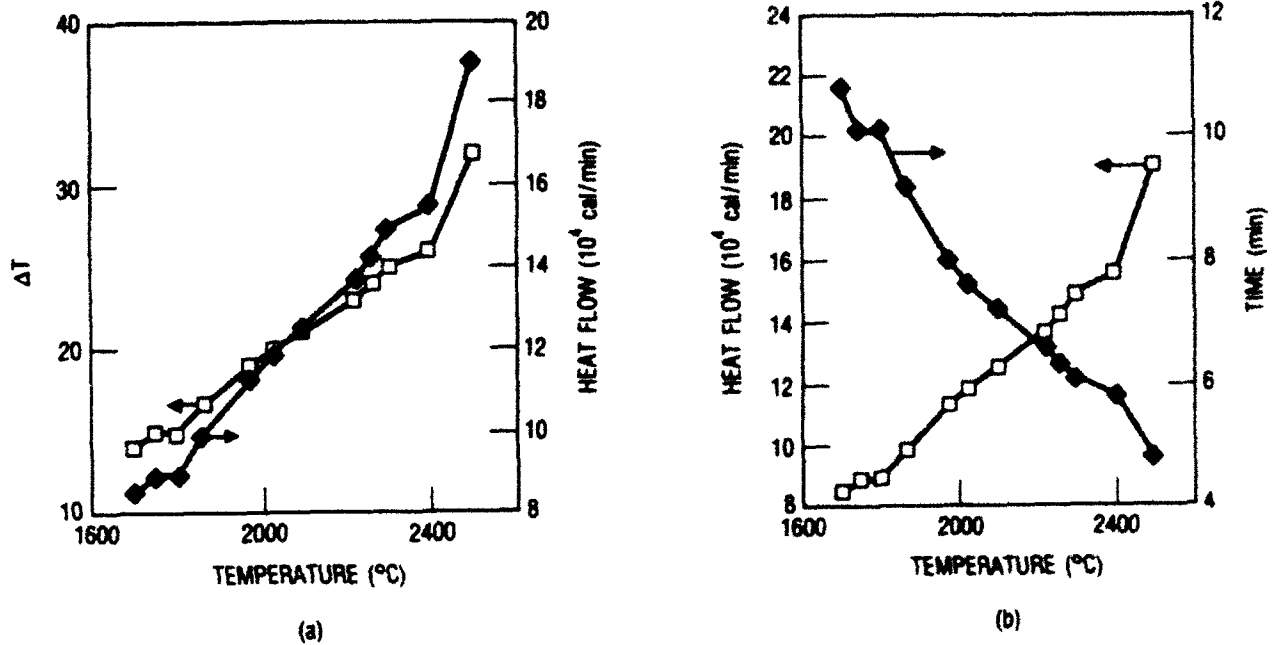


Fig. 2. (a) Heat flow out of furnace case as measured from change in the temperature of the cooling water flowing at a known rate, $\dot{Q} = \dot{m} c \Delta T$: \dot{m} is the cooling-water flow rate, c is the heat capacity of water, ΔT is the temperature rise of the cooling water, and \dot{Q} is the heat flow into the furnace shell from the interior. (b) Approximate times for the exterior of the furnace to reach melting temperature. Note also that these calculations assume constant heat-flow rate, i.e., that the interior of the furnace stays at constant temperature after water interruption, which it does not. The actual time to failure is, however, regarded as 50% shorter than indicated in order to allow a safety margin.

available for the operator to shut down the power so that no potential safety problem is presented. The possibility of a cooling-water failure dictates that furnace operation be carried out only during the normal working shift, limiting run length to about 8 hr. A "tag-team" system is used to ensure the continuous presence of a qualified individual in the laboratory during that shift. Figure 3 is a diagram of the cooling system with the emergency bypass system noted.

Sample dilation and temperature data are recorded simultaneously by a multitasking laboratory computer, a Hewlett-Packard Integral PC. The data from completed runs are sent as ASCII files for analysis to a VAX 11/785 mini-mainframe computer via the Intelligent Data Switch (IDS). The Interactive Data Language (IDL) programming language, used for data analysis on the VAX computer, greatly reduces programming and data analysis time while retaining the inherent flexibility of user-designed data analysis software. The BASIC language code for data acquisition is included in Appendix A, and the IDL code for data analysis is in Appendix B.

The temperature of the furnace and that of the test sample are measured by two different systems: For temperatures below 1000°C, a Chromel-Alumel thermocouple is positioned in the sample cage, just below the sample. For the 900-to-3000°C range, optical pyrometry is used and requires two separate pyrometers: a total-emission-type pyrometer, which covers the range 1000 to 1550°C and measures the total flux of radiation from a specific area of the sample; and a so-called two-color pyrometer, which reads from 1550 to 3000°C and measures the intensity ratio of two adjacent near-infrared wavelengths. For both pyrometers, the sample's emissivity is assumed to approximate that of a blackbody. For maximum accuracy, a small cavity-radiator serves as a target for the pyrometer measurements. The cavity-radiator was used to reduce the undesirable reflectivity that the system may have on the sample so that better accuracy can be achieved. One side of the radiator is located within 1 mm of the sample during the run to maintain near-isothermal conditions. As the furnace temperature passes 1000°C during a typical run, the thermocouple is withdrawn manually. The temperature-measurement function automatically passes from the thermocouple to the optical pyrometers at about 950°C.

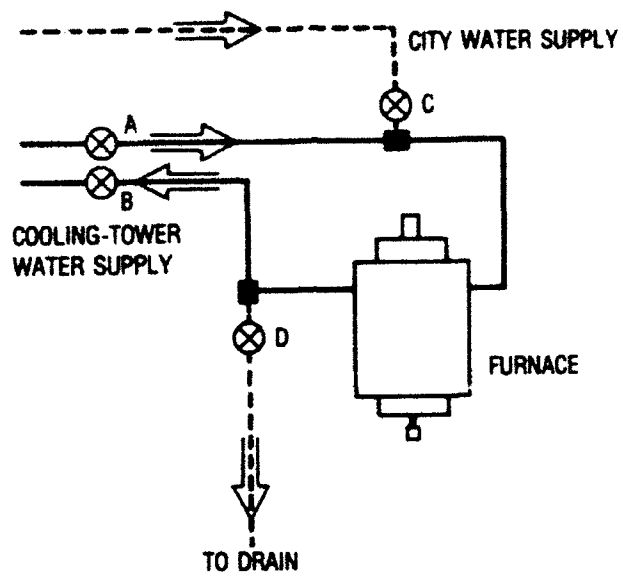


Fig. 3. Diagram of the cooling-tower water system for the dilatometer furnace. If the system fails, valves A and B are closed and valves D and C are opened (in that order) to provide a city-water backup.

The selection of the particular inert purge gas, helium, for the dilatometer is important for very-high-temperature applications with an electric field present. At temperatures above about 2540°C, argon, the most commonly used of the noble gases, begins to ionize and conduct electricity. The location of both electrodes at the same end of the heating element in this particular furnace design results in a large electric potential gradient there (-50 V/cm). When attempts were made to heat the furnace above 2540°C in an Ar atmosphere, a spontaneous short developed across the heating elements and the furnace would cool. The short carried about 300 A at 10 V and was attributed to thermally assisted ionization of the Ar. When helium was substituted in the furnace atmosphere, the short disappeared completely.

The useful upper temperature range of the dilatometer is dictated primarily by the lifetime of the polycrystalline graphite heating element. At 3000°C, the lifetime of the element is less than 30 min; below this temperature, the life of the element increases substantially. Wachi and Gilmartin⁴ found that at high temperatures (>2900°C), the carbon binder phase in a polycrystalline graphite begins to evaporate preferentially, generating gaps between the graphite grains; the graphite grains are then (apparently) ejected from the degrading material. Electric arcs that may form in the resulting gaps in the dilatometer heating-element material might also accelerate the erosion process. The service life of the heating element when the furnace is run to 3000°C is about three weeks, and that of the furnace retort is about three months. Upper temperatures are therefore usually limited to 2850°C.

III. CALIBRATION OF THE INSTRUMENT

A. THEORETICAL

The accuracy of the single-pushrod dilatometer design is limited by the thermal expansion of the materials out of which the dilatometer is fabricated. Vitreous silica is the preferred material for high-precision dilatometers because, for many applications, its coefficient of thermal expansion (CTE) contributes negligibly to the overall expansion of the sample/dilatometer system. However, vitreous silica dilatometers must be corrected for high-accuracy measurements on materials whose thermal expansions are close to that of silica glass itself (about $5 \times 10^{-7} \text{ }^\circ\text{C}^{-1}$). Silica cannot be used in this dilatometer, however, because the useful maximum temperature for silica is only about 1100°C . The dilatometer discussed here, therefore, is constructed of a fine-grained polycrystalline graphite (SPEER, Inc.) to permit high temperatures to be investigated. The average CTE of such graphites ranges from about 3 to $7 \times 10^{-6} \text{ }^\circ\text{C}^{-1}$ from room temperature (RT) to 3000°C , which is about an order of magnitude greater than that of silica. Consequently, the dilatometer must be carefully calibrated to remove the apparent CTE contribution of the probes in the sample pushrod/tube assembly.

The procedure we used for correcting the dilatometer data arises from the mechanics of the dilatometer system and is generalized for single-pushrod dilatometers; it will now be described. Thermal strain occurs at specific locations in the dilatometer, as indicated in Fig. 4a. For simplicity, the figure includes only the primary structural parts of the dilatometer. The three-point-bend fixture, which replaces the dilation sample in the hot zone for flexural studies, is shown in Fig. 4b. The same correction procedure can be used in the flexure mode if an inflexible standard sample, such as pyrolytic graphite, is used for the calibration.

The sample and the part of the pushrod/tube assembly that are in the hot zone are heated during a test and undergo thermal strain. The total strain is measured by the LVDT at C. The contribution of the "overlapping"

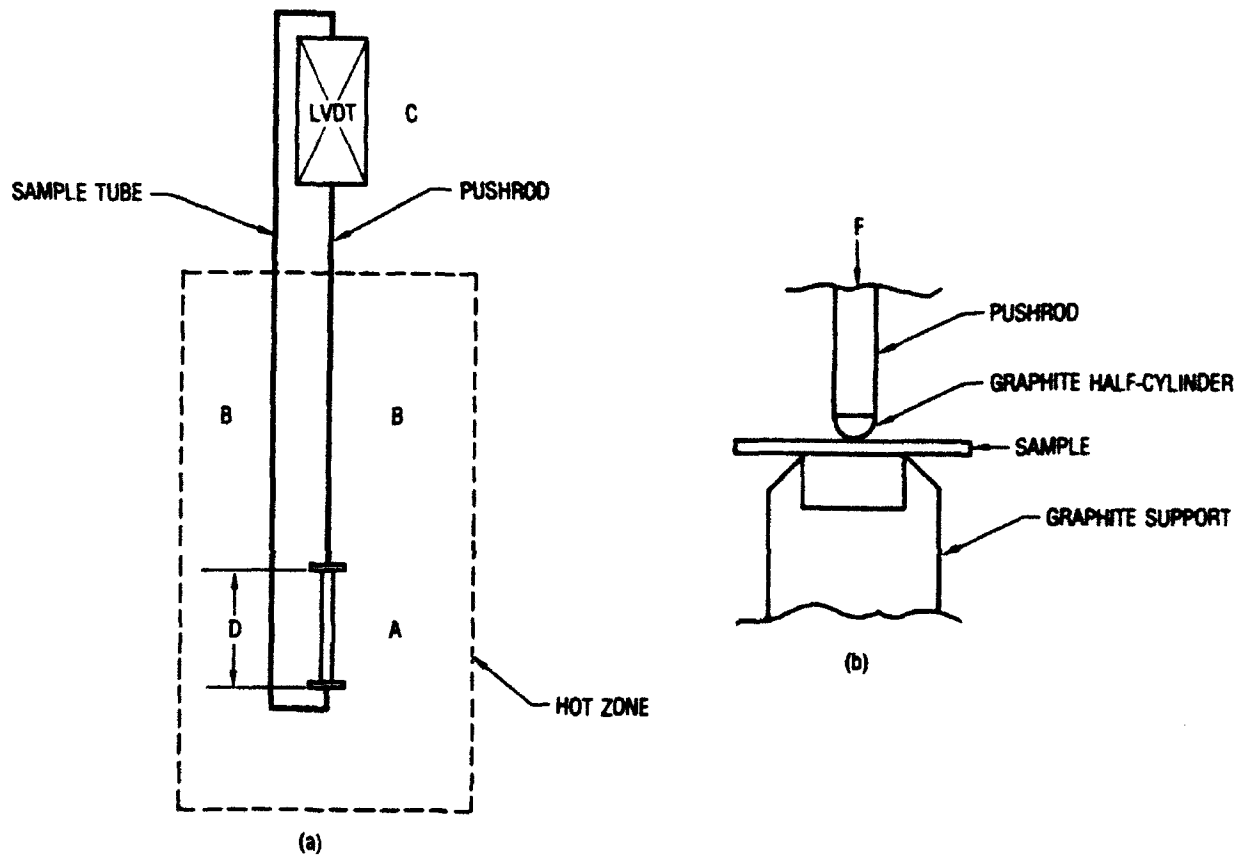


Fig. 4. (a) Schematic of single-pushrod dilatometer.
 (b) Detail of three-point-bend fixture. (F is force.)
 During use, the fixture is positioned in sample zone A
 of (a).

portion of the probes (in region B) to the total measured strain is zero if the materials that compose them are identical in thermal expansion, and if the temperature gradients along the tube and the pushrod are the same. However, the thermal strain of the tube and pushrod do not cancel in the region where the sample is located (D); the thermal strains from both the sample (A) and the sample tube in region D contribute simultaneously to the net thermal strain measured at the LVDT. Therefore, the LVDT actually measures the thermal strain difference between the sample length, A, and the corresponding length of the sample tube, D. The arrangement of the probes requires that the thermal strain of the length of the sample tube in region D be added algebraically to the total measured thermal strain, because the strain of this part of the tube acts to move the center of mass of the sample downward, away from the LVDT. The thermal strain characteristic of the sample tube, at least in the region overlapped by the sample, must first be precisely known before this can be done.

The characteristic uniform thermal strain of the sample tube should be ascertainable by measuring the thermal strain of a well-characterized reference material. However, it was found that the thermal strain of the graphite sample tube could not be normalized with respect to change in the sample length (see Fig. 7). Therefore, measurements of a single reference sample of fixed length were not adequate to characterize the tube for all sample lengths. (The correction for this effect will be discussed in the next section.) The difficulty appears to be due to the large and unequal thermal gradient in the sample tube and pushrod at the edge of the hot zone, and the fact that different lengths of the pushrod enter the hot zone for different sample lengths.

To bypass this problem without extensively characterizing the baseline associated with various sample lengths, the sample length was standardized at 1 cm. The measured strain at the LVDT, then, can be thought of as the sample strain plus the dilatometer's instrumental response:

$$\epsilon_{\text{NET SAMPLE}} = \epsilon_{\text{SAMPLE}} + \epsilon_{\text{MACHINE}} \quad (1)$$

which can be rewritten

$$\alpha_{\text{SAMPLE}}^{\text{NET}} = (\alpha_{\text{SAMPLE}} - \alpha_{\text{STD}}) + \alpha_{\text{STD}} + \alpha_{\text{MACHINE}} \quad (2)$$

where α_{STD} is the known expansion of a standard reference material. A sample of the standard reference material can be run in the dilatometer, yielding, by Eq. (1),

$$\alpha_{\text{STD}}^{\text{NET}} = \alpha_{\text{STD}} + \alpha_{\text{MACHINE}} \quad (3)$$

The net strain of the standard ($\alpha_{\text{STD}}^{\text{NET}}$) can be subtracted from that of the unknown, Eq. (2), to yield

$$\alpha_{\text{CORRECTED}}^{\text{NET}} = \alpha_{\text{SAMPLE}} - \alpha_{\text{STD}} \quad (4)$$

Since α_{STD} was assumed to be known, it can be added (as previously mentioned) to this result to yield the true thermal strain of the unknown sample.

The material for a standard sample should be selected because it is either precisely characterized or it possesses a low enough CTE that any imprecision in the characterization of its CTE is of little significance. Practical candidates are silica (fused quartz glass), Zerodur-type glass ceramics ($5 \times 10^{-8} \text{ }^\circ\text{C}^{-1}$), and titanium silicates ($< 5 \times 10^{-7} \text{ }^\circ\text{C}^{-1}$). Partially crystallized glasses, such as Zerodur, are limited to about 600°C . Silica can be subjected to almost 1100°C and can be made more refractory and lower in CTE by the addition of up to 10% titania (ULE).⁵ The melting ranges of titanium silicate glasses have not been clearly identified in our laboratory, but such glasses appear to withstand temperatures of about 1400°C without melting, although devitrification occurs at the sample surface. In general, the above materials offer such low expansions that even an error as large as 50% in their CTE data represents an order-of-magnitude-lower error than is expected from the graphite dilatometer. (Silica-based, single-pushrod dilatometers of this type are

practically limited to measurements of the order of 10^{-6} m due to mechanical errors in the apparatus.⁶) National Bureau of Standards (NBS, now referred to as NIST, National Institute of Standards and Technology) standard reference material (SRM) 738 (sapphire), which is no longer available from NIST, can also be used since it is very accurately calibrated, but its temperature range is limited to about 1550°C.

B. PRACTICAL ASPECTS OF DILATOMETER CALIBRATION

Polycrystalline graphite has a very high use temperature, and consequently it has been employed as a standard material, in other work, after careful optical calibration.⁷ However, pyrolytic graphite (PG) has a lower CTE that is considered to make it a better standard material because errors in estimating its CTE would be correspondingly low. The theoretical (crystallographic) expansion of graphite parallel to the basal plane is about that of silica ($1 \times 10^{-6} \text{ }^\circ\text{C}^{-1}$), a fact that favors its selection; however, owing to the crystalline imperfections inherent in PG, an expansion about two times higher than this is usually observed.

For the above reasons, a standard PG sample was used in this dilatometer and was developed in-house as follows. A 7-cm-long sample of PG was pre-annealed at 2750°C for 2 hr in a graphite tube furnace, then reheated; its thermal strain was measured optically (above 850°C) using traveling telemicroscopes that were sighted on fiducial marks in the ends of the rod. A 1-cm piece was excised from this sample for use as a standard. It was then calibrated to 750°C in a DuPont 943 thermomechanical analyzer (silica dilatometer), which was referenced to NBS silica (SRM 739). These thermal strain data were then consolidated to yield the thermal strain behavior of the sample over the entire temperature range of the dilatometer. A polynomial curve was then fit to the data for use in subsequent data analysis. Figure 5 plots the data from this standard and the polynomial fit. Published data for the thermal strain of ATJ-S polycrystalline graphite are plotted in curve (b), Fig. 5, for reference.⁸

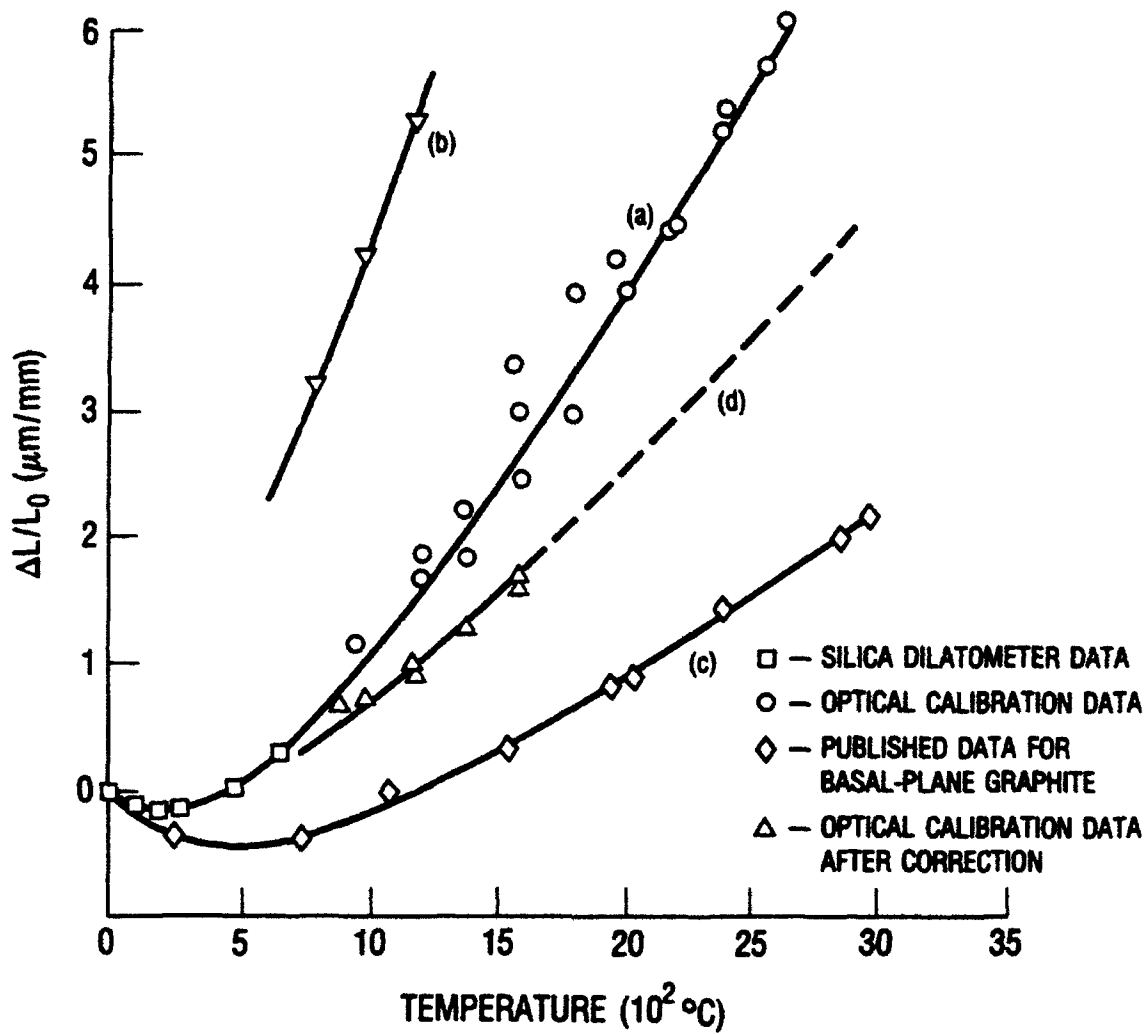


Fig. 5. Thermal strain data from (a) optical calibration of the in-house-developed pyrolytic graphite standard, (b) published data for ATJ-S polycrystalline graphite,⁶ and (c) theoretical basal-plane expansion of graphite. The dashed curve (d) is the corrected PG data from the in-house standard.

Measurements of the NBS 738 sapphire sample in the dilatometer after this calibration procedure indicated the need for applying the following correction to the optical calibration data for the PG standard. The CTE data for a sample of NBS 738 sapphire, together with the published data,⁹ are plotted in Fig. 6. None of the materials involved, in either the standards or the equipment, undergoes phase changes during heating, and all are considered homogeneous and isotropic. Therefore, it was assumed that these materials display expansion characteristics described by a function that is continuous, strictly increasing, and has first and second derivatives that are also continuous and strictly increasing (i.e., the curve is very "smooth," having no inflections). This is a good assumption since graphite is nonpolymorphic at the temperatures and pressure used, and pre-heat treatment to high temperatures renders it stable at lower temperatures.^{10,11} In order to make these smoothness assumptions, the dilatometer had been preconditioned by heating to 3200°C for 0.5 hr prior to calibration.

The deviation of the measured sapphire standard data from the published data increased very smoothly (see deviation data in Fig. 6a), thereby indicating that a linear error was present in the optical calibration data of the PG standard. The indicated correction for this deviation was made to the optical calibration data by extrapolating the deviation to 3000°C and subtracting the resultant curve from the PG-standard data (Figs. 5 and 6).

To observe the dilatometer's fine-scale instrumental response, samples of ATJ-S polycrystalline graphite were measured in the dilatometer. Because the probes are also made of polycrystalline graphite, the net thermal strain measured by the LVDT was predicted by Eq. (1) to be \approx zero except for such fine-scale nonlinearities. Uncorrected [i.e., Eq. (1)] expansion curves that illustrate this behavior were obtained from three ATJ-S graphite samples of different lengths from the same block of graphite and are plotted in Fig. 7. Because the thermal expansion of the graphite in the samples and probes is assumed to be very smooth, the inflected shape of the curve is attributed to interaction of the thermomechanical and

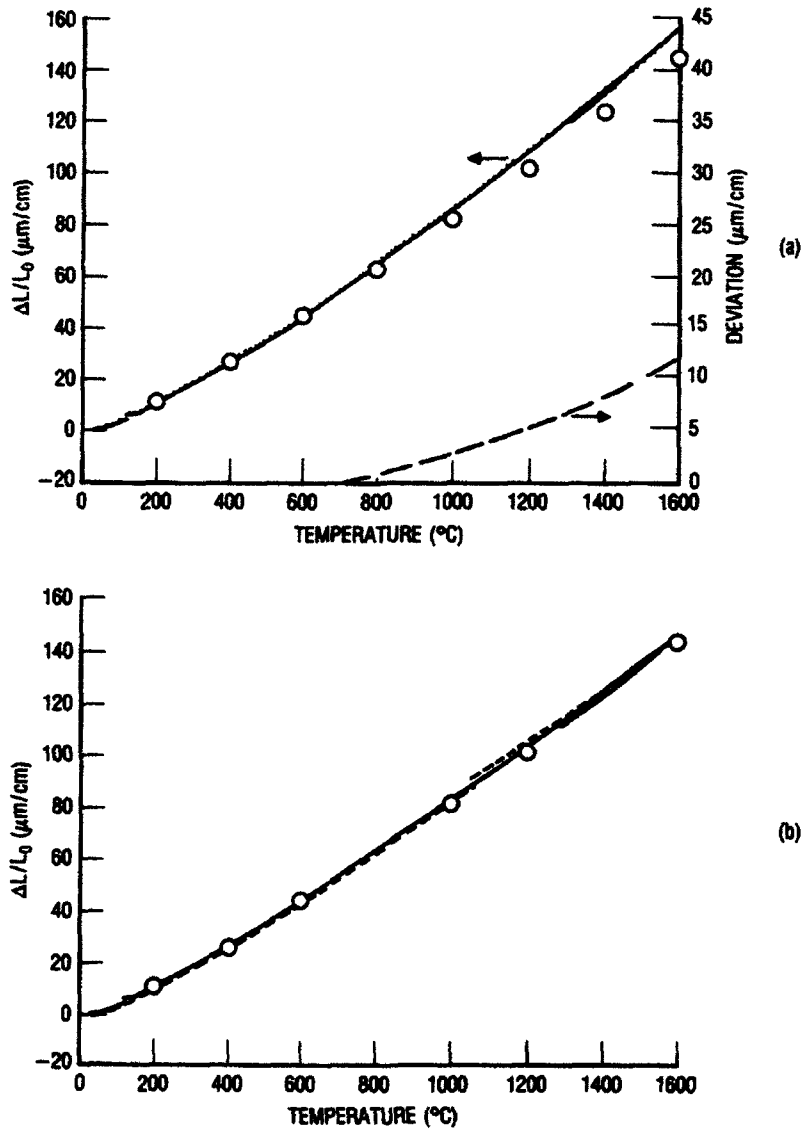


Fig. 6. (a) Initial dilatometer measurement, following calibration, on NIST sapphire standard reference material SRM 738 (solid line). The published data for this material are displayed pointwise as open circles. The deviation between measured and published data is also shown (dashed line). The indicated error is in the optical calibration data ($> 700^{\circ}\text{C}$). (b) Two successive runs on SRM 738 after subtracting deviation data (extrapolated to 3000°C) from graphite-standard calibration curve. (See also Fig. 5.) Published data for SRM 738 are also shown, as open circles.

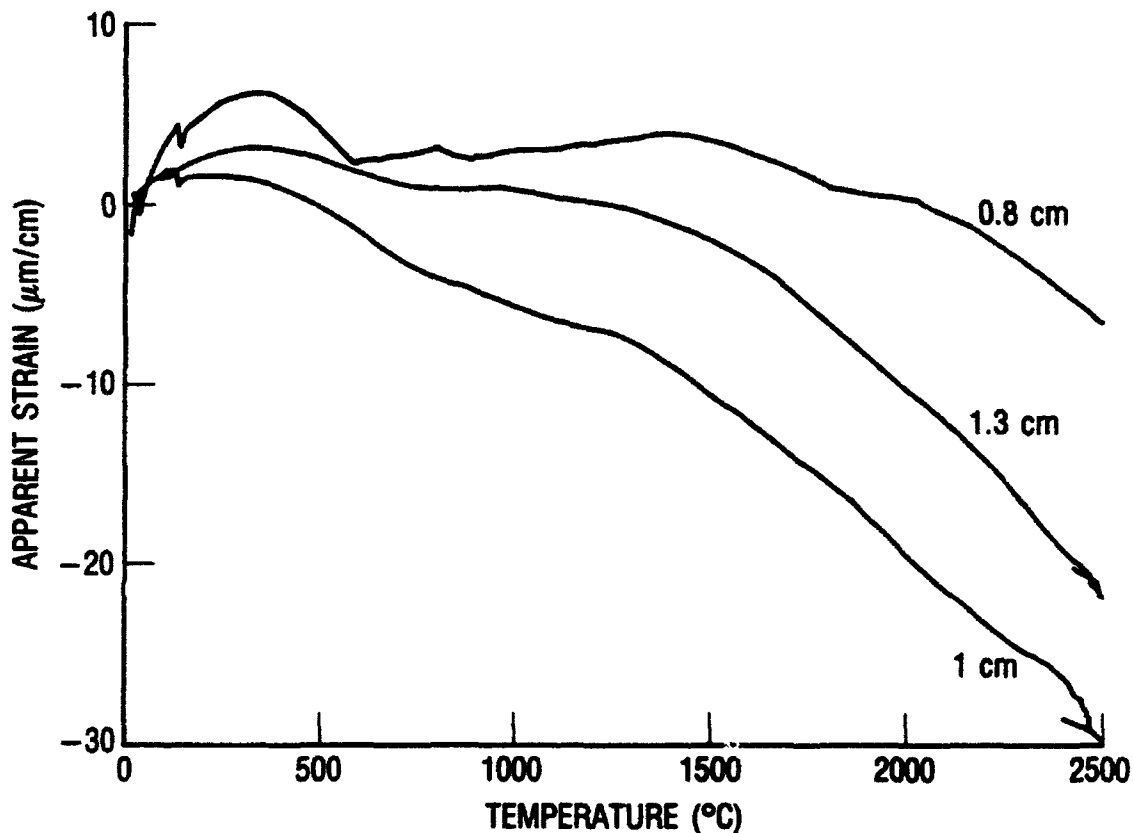


Fig. 7. Thermal expansion data for ATJ-S polycrystalline graphite samples of different lengths. Since the ATJ-S graphite has almost the same CTE as the sample tube/pushrod assembly, the uncorrected data have a small net slope. The inflections present in the curves are attributed to the instrumental response of the dilatometer, since the samples and the sample probes undergo no phase changes during heating. The dilatometer's response to changes in sample length is nonlinear and not monotonically varying with respect to sample length. The length of sample for each curve is indicated.

electronic systems in the dilatometer. Although it varies with sample length in a complex manner, the fine-scale instrumental response can be considered constant if the sample length varies only by the amount typically associated with the thermal strain of high-temperature materials ($<20 \times 10^{-6} \text{ }^\circ\text{C}^{-1}$). [For very large strains, such as those associated with pyrolyzing carbon precursor materials (see Fig. 12), fine-scale nonlinearities can be neglected.] Such nonlinearities are included in the instrumental response term [Eq. (3)] by using a higher-order polynomial function to fit the data prior to subtraction, and a seventh-order polynomial fit was found to be adequate. The room-temperature sample length also must be held constant; we therefore standardized the room-temperature sample length at 1 cm. Based on the data shown in Figs. 5 and 6, the resolution of the system is better than $\pm 5 \text{ } \mu\text{m}$, giving a typical sensitivity of about $0.5 \times 10^{-6} \text{ }^\circ\text{C}^{-1}$.

The above rationale and data-correction procedures are also applied to analyze data from dilatometer runs with bar samples in the flexure mode, using the arrangement shown in Fig. 4b.

IV. RESULTS

In this section we briefly describe the results from early runs of the dilatometer to illustrate the utility and flexibility of the system. The discussion is also intended to inform about the general thermal strain behavior of carbonaceous materials.

Uncorrected data, representing the net thermal strain of the dilatometer-sample system [Eq. (1)], are presented in Fig. 8 for non-heat-treated PG and the PG standard sample. The slope is negative because the sample data are uncorrected. The progressive stabilization of the PG (which is manufactured at about 2400°C) and the expansion of the PG standard (which had been pre-annealed at 2750°C) are indicated. The magnitude of the sharp, irreversible increase in the basal-plane dimension of the non-heat-treated sample diminishes progressively as crystalline defects are annealed out and the degree of graphitic order of the sample approaches a limiting value¹⁰⁻¹² with increasing time at high temperature. The CTE of the pyrolytic graphite in the basal plane changes little as a result of the high-temperature heat treatment, indicating good stability of the sample's CTE with respect to use of the standard at high temperature.

Typical expansion data taken from various carbon materials are shown in Figs. 9 and 10. The true (corrected) data taken both perpendicular and parallel to the basal plane of a sample of pyrolytic graphite, Fig. 9, exhibit the large thermal strain anisotropy characteristic of graphite, as well as the irreversible strains associated with further-graphitizing heat treatment, past the original temperature of manufacture.¹⁰ The data in Fig. 10 are for representative samples of the three principal weave geometries of C-C composites: one-, two-, and three-dimensional weaves. They are very similar in CTE because their thermal strains are dominated by their constituent carbon filaments, which vary in CTE by only about a factor of 2 from that of basal-plane graphite.¹¹

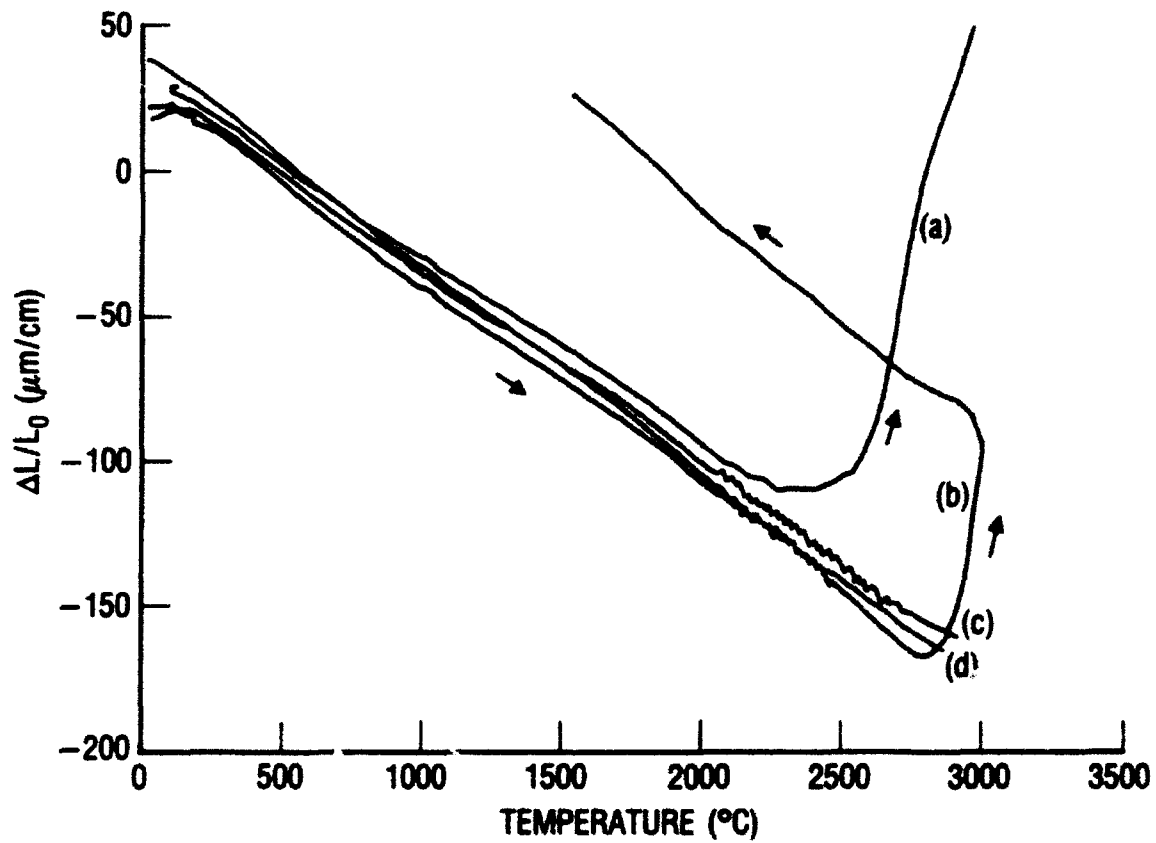


Fig. 8. Uncorrected thermal strain data from pyrolytic graphite. Curves (a) and (b) are from successive runs on as-received samples; curves (c) and (d) are from the in-house-calibrated standard. The CTE of the pyrolytic graphite (excluding its initial high-temperature pyrolysis expansion) is relatively constant even after the large (irreversible) strains that accompany the initial heatings above the temperature of manufacture (about 2400°C).

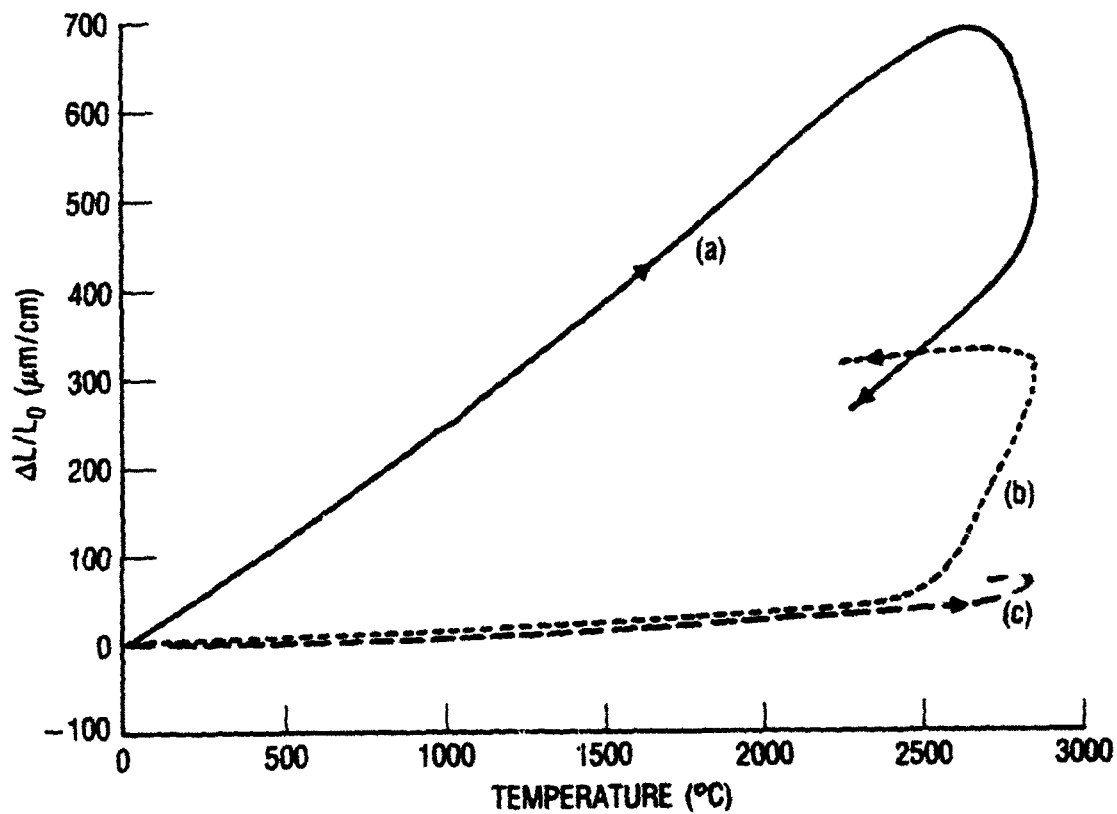


Fig. 9. True thermal strain response of pyrolytic graphite in (a) basal-plane-normal direction (c-axis) for the second run, and (b) and (c), parallel to the basal plane (a-axis) for the first and second runs, respectively. The irreversible shrinkages and expansions occurring in the c- and a-axes above 2500°C are associated with further graphitization.⁹ Curve (c) indicates that the sample becomes stable with respect to thermal strain after sufficient heat treatment.

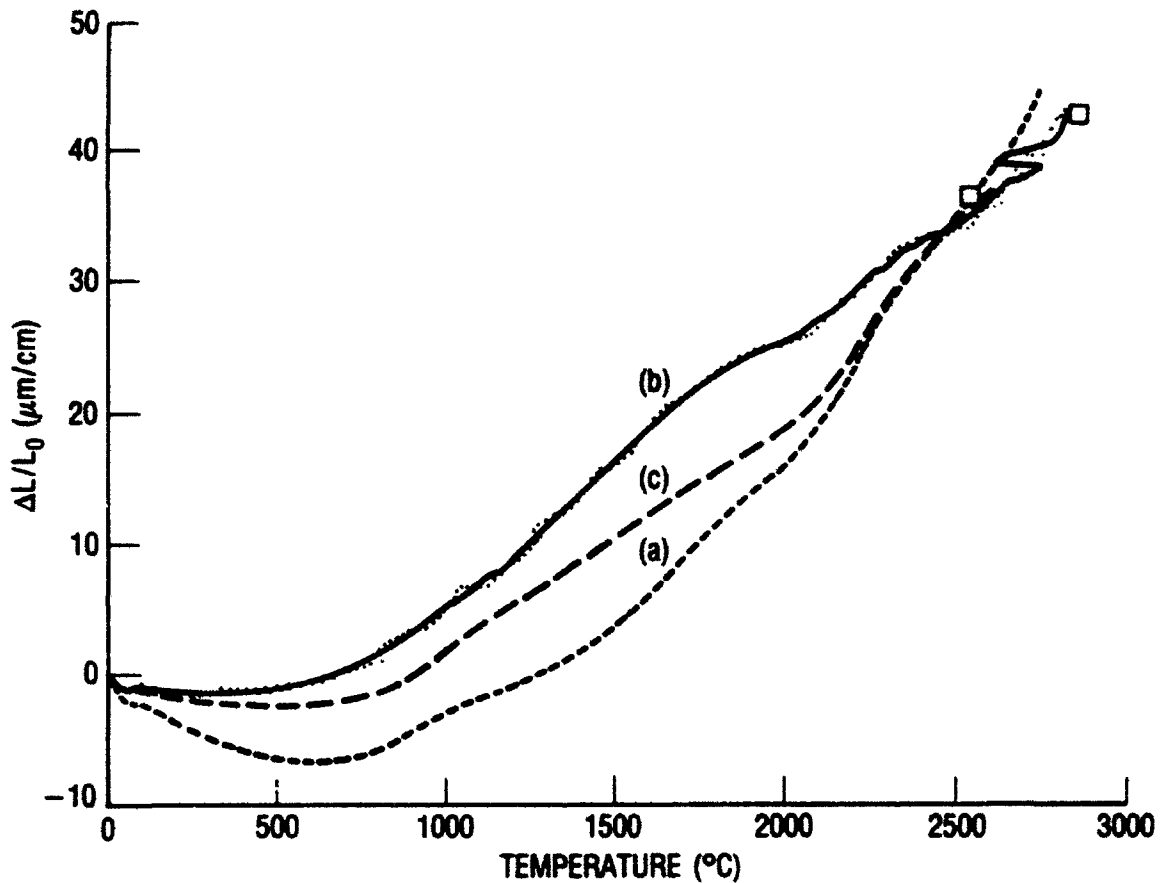


Fig. 10. Thermal strain of several carbon-carbon composite configurations: (a) a Cartesian 223 weave three-dimensional composite manufactured by General Electric; (b) a unidirectional C-C composite made with T300 fibers and pitch-derived graphite matrix; and (c) a two-dimensional composite made from satin weave P100 fibers in a pitch-derived graphitic matrix.

As previously mentioned, the dilatometer can also be run in the three-point-bend mode. In this arrangement, the sample is in the form of a bar $0.8 \times 2.4 \times 5$ mm (length). The pushrod is placed on the center of the span to record the inelastic deflection as a function of temperature. Those elastic deflections that occur are of the order of a few microns and are neglected. This type of test is somewhat uncommon; therefore, it is appropriate to indicate the general type of data yield.

The inelastic strain of samples of pyrolyzing PAA, phenolic, and polyfurfural alcohol during heat treatment is shown in Fig. 11. The strain behavior reveals that there are two temperature ranges in which significant amounts of strain energy are absorbed by the samples. The first occurs at low temperatures, essentially from the cure temperature to about 1000°C , and relates to the formation of the polymeric carbon submicrostructure.¹³ The second range occurs above about 2000°C , where graphitization is initially observed in the (formerly glassy) matrices of C-C composites, up to the temperature limit of the dilatometer. Macroscopic work absorption in this range is probably associated with creep and grain-boundary sliding processes.^{12,13} Such observations are important in research on carbonization and graphitization processes. For further information, the reader is referred to the literature.

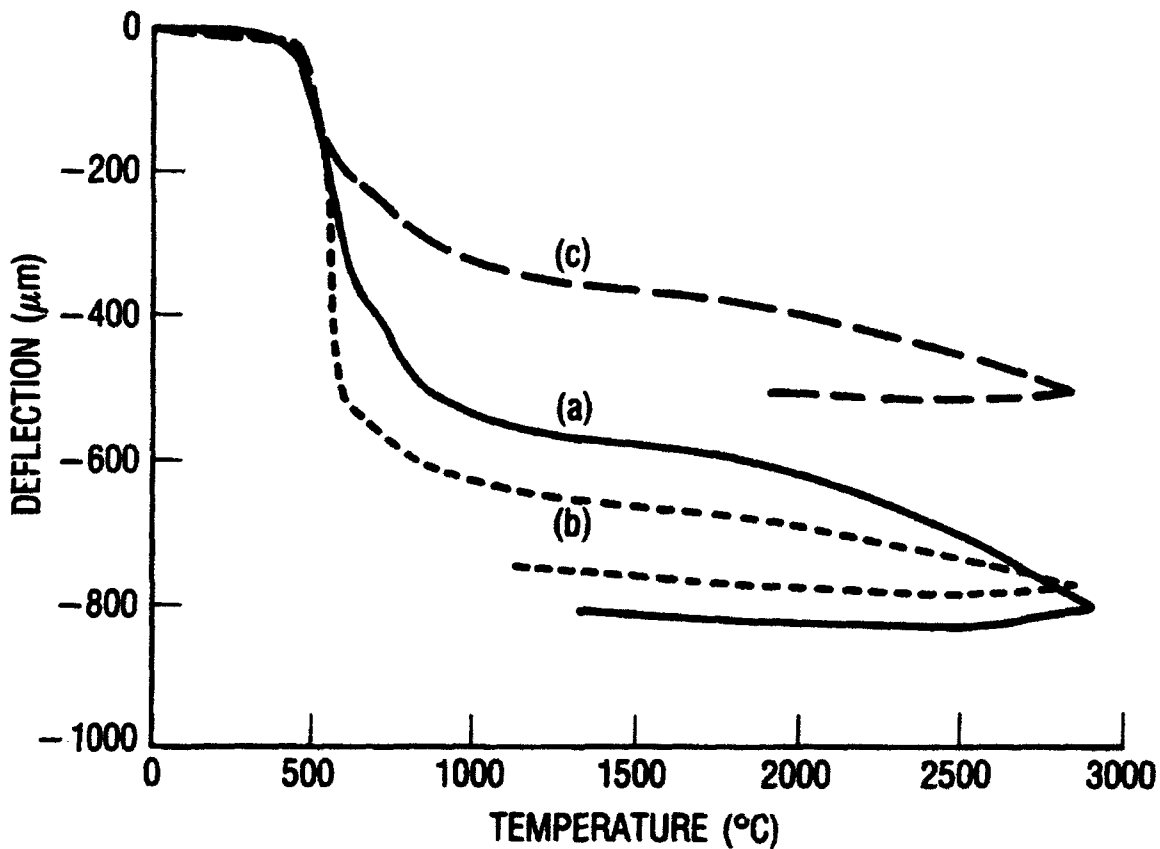


Fig. 11. Data from three-point-bend samples of (a) PAA, (b) phenolic, and (c) furfural resin samples that were precured to 350°C. The maximum shear and outer-fiber tensile stresses were 3.5 KPa and 0.25 MPa, respectively. The data indicate that the three carbons differ in the amount and temperature range of strain-energy absorption. Phenolic resin absorbs more strain energy during the early stages of pyrolysis; PAA absorbs more at graphitization temperatures (>2000°C); and furfural resin carbon absorbs less at all temperatures.

V. CONCLUSIONS

The dilatometer system described here can measure the thermally induced strain (deflection) of samples to a precision of better than $\pm 5 \mu\text{m}$ from room temperature to 3000°C . This precision is achieved by characterizing the instrumental response of the system for a known standard that can be referenced to NBS (NIST) data, then algebraically subtracting that functionality from the strain of the unknown sample. The dilatometer thus emulates a virtual two-pushrod dilatometer system. Using computer data acquisition and analytical methodology makes quantifying a sample's thermodynamic responses a very rapid process.

Nonthermodynamic properties, such as the strains occurring in carbonaceous materials during their pyrolysis, can also be measured. Differences in the pyrolysis behavior of carbon precursors have been observed. It is proposed that characterizing and analyzing such differences may shed light on the behavior of precursors in the matrix of C-C composites and the effects of the precursors on the bulk thermal strains of such composites.

REFERENCES

1. R. A. Meyer et al., Strategic Missiles Materials Technology (SMMT) Program Carbon-Carbon Composite Technology, Report No. TOR-0082(2726-01)-2, The Aerospace Corporation, El Segundo, CA (1982).
2. Handbook of Chemistry and Physics, 64th ed., eds. R. C. Weast et al., CRC Press, Boca Raton, FL (1984).
3. J. Jortner, "Macroporosity and Interface Bonding in Multi-Directional Carbon-Carbons," Carbon 24, 603-13 (1986).
4. F. M. Wachi and D. E. Gilmartin, High Temperature Mass Spectrometry, Free Vaporization Studies of Graphite, Report No. TR-0200(4250-40)-6, Vol. I, The Aerospace Corporation, El Segundo, CA (1969).
5. P. C. Schultz, "Binary Titania-Silica Glasses Containing 10-20 Wt.% TiO₂," J. Am. Ceram. Soc. 59 (5-6), 214 (1976).
6. E. Wolff, "Materials and Processes - In Service Performance," Natl. SAMPE Tech. Conf. Series Vol. 9, 57-72 (1977).
7. J. R. Koenig and C. D. Pears, Evaluation of Four GRAPHNOL Materials, Report No. SoRI-EAS-74-328, Southern Research Institute (1975).
8. H. S. Starrett and C. D. Pears, Probable and Average Properties of ATJ-S(W) Graphite, AFML-TR Vol. 1, AFML/MXS, WPAFB, OH (1972).
9. American Institute of Physics Handbook, 3rd ed., ed. D. E. Gray, McGraw-Hill (1986).
10. A. Oberlin, "Carbonization and Graphitization," Carbon 22, 521-41 (1984).
11. E. Fitzer, Distinguished Lecture Series, MTC Southern Illinois University, Carbondale, IL (1986).
12. Y. Hishiyama et al., "Graphitization of Carbon Fiber/Glassy Carbon Composites," Carbon 12, 249-58 (1974).
13. G. M. Jenkins, K. Kawamura, and L. L. Ban, "Formation and Structure of Polymeric Carbons," Proc. R. Soc. London, Ser. A. 327, 501-17 (1972).

APPENDIX A.

DILATOMETER DATA ACQUISITION PROGRAM

The following BASIC language code runs on a multitasking Hewlett-Packard personal computer under a BASIC Shell in the UNIX environment. It is used for laboratory data acquisition.

```

10 !*****
20 !
30 !   ASTRO Furnace data acquisition program
40 !
50 !           Jun 16 1987 (Vers 2.1)
60 !
70 !
80 !           Makes a daughter file in /usr/ASTRO
90 !           which can be read by unix for VAX transfer
100 !
110 !*****
120 SHORT minT,maxT,interv,timee,hrt,thick,sthick,zero @ INTEGER nopoints
    @ point=1
130 CLEAR @ ALPHA 0,0 @ DIM sampl$(80)
140 DISP @ DISP @ DISP @ DISP
150 DISP "   Astro Furnace Data program" @ MASS STORAGE IS "/usr/ASTRO"
160 DISP @ ASSIGN 16 TO "astro!.dat.tmp"
170 DISP "   calibrate LVDT [y/n]"
180 INPUT yesno$ @ PRINTER IS 16
190 IF yesno$="n" OR yesno$="N" THEN GOTO 220
200 GOSUB 990
210 GOTO 350
240 GOTO 330
330 DISP @ DISP @ DISP "   enter cal factor (V/um)"
340 INPUT calfac @ zero=0
350 DISP @ DISP @ DISP
360 DISP "   Enter heating rate (C/min.)"
370 INPUT hrt
380 DISP @ DISP "   Enter File name"
390 INPUT name$
400 z1=LEN(name$)
410 datee$=DATE$
420 DISP @ DISP "   Sample I.D. "
430 INPUT sampl$
440 DISP @ DISP "   Enter sample thickness (mm)"
450 INPUT sthick
460 DISP @ DISP "   Enter min,max temperatures (C)"
470 INPUT minT,maxT
480 DISP @ DISP "   Enter sample interval (seconds)"
490 INPUT interv
500 DISP @ DISP @ DISP "   Length of run (minutes)"
510 INPUT timee
520 timeee=(maxT-minT)/hrt !   time length of run !!!!
530 DISP @ DISP "   Time to maximum temp: ";timeee @ DISP
540 nopnts=INT(timee/(interv/60)) !   total # of data points in run !
560 GOSUB 890 !*****start file*****!
570 DISP @ DISP @ DISP @ DISP " to start run, Press f1"
580 ON KEY# 1," start" GOTO 600
590 GOTO 590
600 OFF KEY# 1 @ DISP @ DISP "starting" @ DISP @ DISP
    @ DISP " Point   time   temp   LVDT"
610 ON KEY# 2," HOLD" GOTO 1380
620 time=TIME !   starting seconds since midnight !
630 datt=DATE-87000 ! starting # of days since start of year
640 !!!!!start of data loop!!
650 !
660 ON ERROR GOTO 690
670 ASSIGN 7 TO "hpib.b2"
680 OFF ERROR @ GOTO 695

```

```

1290 OUTPUT 709 ; "AC5" ! #####
1300 ENTER 709 ; c1,c2,c3,c4,c5,c6,c7,c8,c9 ! #####
1310 calfa(LL)=((c1+c2+c3+c4+c5+c6+c7+c8+c9)/9-zero)/thick ! V/um #####
1315 WAIT 1000 ! #####
1320 NEXT LL ! #####
1330 calfac=(calfa(1)+calfa(2)+calfa(3))/3 ! #####
1340 ASSIGN 7 TO "*" ! #####
1350 DISP @ DISP " Cal. factor=";calfac @ RETURN ! #####
1360 !-----#####
1370 !-----#####
1380 DISP @ DISP @ DISP " ...holding, end=f3; continue=f4"
1390 ON KEY# 3," end" GOTO 860 @ ON KEY# 4," cont." GOTO 1410
1400 GOTO 1400
1410 OFF KEY# 3 @ OFF KEY# 4 @ GOTO 840
1420 recover:
1430 DISP " A Timeout has Occurred on 701... Recovering"
1440 ASSIGN 7 TO "*"
1450 GOTO 650

```


APPENDIX B.

DILATOMETER DATA ANALYSIS PROGRAM

The following IDL^{*} language code is run on a VAX 11/785 computer to analyze the data collected in the laboratory. Data are transferred to the VAX via Kermit file-transfer software (public domain).

^{*}Interactive Data Language, RSI, Inc., 2021 Albion St., Denver, CO.

```

SET PLOT,0
VT100
!FANCY=0           ; Version 5.00 pyrostd baseline 7th polynomial
                   ; JAN 10, 1989 with SMOOTHING
                   ;   and SCATTER PLOT and AUTOREAD
                   ;   and DERIVATIVE and LEGANDS

PVAR=''
print,' ASTRO FILE DATA PLOTTER; OVERPLOTED FILES WILL BE OVERLAYED IN THE'
PRINT,' ORDER GIVEN.  SCALE WILL BE THAT OF THE FIRST FILE GIVEN.'
PRINT,' Be sure that the terminal is in CAPITAL letter mode!'
PRINT,' '
PRINT,' with SMOOTHING and SCATTER PLOT'
PRINT,' '

NUMP=10
PRINT,' Enter # of points to be averaged for smoothing'
read,NUMP
PRINT,' '
PRINT,' NUMBER OF FILES TO BE PLOTTED ?   (<9)'
AB=2               ; NUMBER OF FILES
Z=1                ; A FLAG
READ,AB
CODE=1

ORD=2
PRINT,' '
PRINT,' Plot a polynomial fit to the data? [Y/N]'
read,PVAR
PRINT,' '
IF PVAR EQ 'Y' THEN BEGIN
PRINT,' WHAT POLYNOMIAL ORDER ?'
READ,ORD
ENDIF
PRINT,' '
PRINT,' X-AXIS           Y-AXIS           CODE '
PRINT,' _____'
PRINT,' Temperature      Expansion          1'
print,' Time             Expansion          2'
PRINT,' Time             Temperature        3'
PRINT,' Temperature      Derivative (Temp.)  4   (for dilation)'
PRINT,' Time             Derivative (Time)   5   (for dilation)'
PRINT,' Temperature      Deflection          6   (for flexure)'
PRINT,' Temperature      Deflection          7   (for compression)'
PRINT,' Temperature      Derivative          8   (for compression)'
PRINT,' Temperature      Derivative          9   (for flexure)'
CODE=2

PRINT,' '
PRINT,' Enter CODE'
print,' '
READ, CODE

NUM=INDGEN(AB)
NAME=STRARR(20,AB)
NAME= ''           ; VECTOR OF POINT NUMBERS
                   ; CORRESPONDING VECTOR OF NAMES

YSNO=''
READ,'Display the Directory ',YSNO

```

```

        IF YSNO EQ 'Y' THEN SPAWN, 'DIR'
NUMEE=5

FOR I=1,AB DO BEGIN
    PRINT, 'ENTER NAME OF FILE '           ; get names of files to be plotted
    READ, NAMEE
    NAME(I-1)=NAMEE
endfor

STD1=[-4.35479E-15,4.77169E-12,-1.90235E-9,3.18491E-7,-1.44959E-5,-1.18590E-3,-.44418,1.34
; BASELINE FIT DATA JUN. 25, 1988
STD2=[-3.95873E-16,3.98258E-12,-1.56485E-8,3.14101E-5,-1.35172E-2,.31399]
; COEFF'S FOR GRAPHITE IN BASAL PLANE
STD3=[6.66491E-15,-5.51405E-11,1.69794E-7,-2.40729E-4,0.13016]
; BASELINE FOR COMPRESSION SAMPLE

for i=1,ab do begin
    OPENR,1,NAME(I-1)                       ; do plotting...
    A=STRARR(30,1)
    B=STRARR(60,1)
    C=FLTARR(4)
    D=''
    E=DOUBLE(FLTARR(4,2000))                ; MAKE DATA VECTOR DOUBLE PRECISION

    ON IOERROR,POINTS
    READF,1,A,B,C,D,E
    POINTS: PRINT,(MIN(WHERE(E EQ 0)))/4,' POINTS READ'
    ON IOERROR,NULL
    PRINT,' Number of Data Points to be Plotted ?'
    READ, NUMEE
    NUM(I-1)=NUMEE
    CLOSE,1

    X=E(2,0:NUM(I-1))                       ; DEFINE NEW VARIABLES AND SET UP PLOT
    Y=E(1,0:NUM(I-1))                       ; MICRONS
    XT=E(3,0:NUM(I-1))                      ; TIME

    PYROFLX=(-6.6E-3)*X                     ; FOR FLEX SAMPLES

    Y=Y-(Y(0)+Y(1)+Y(2))/3                 ; SET Y(R.T.)=0

    X=X/8
    Y1=STD1(0)*X^7+STD1(1)*X^6+STD1(2)*X^5+STD1(3)*X^4+STD1(4)*X^3+STD1(5)*X^2+STD1(6)*X+STD
; MAKE BASELINE DATA
    X=X*8
    Y2=STD2(0)*X^5+STD2(1)*X^4+STD2(2)*X^3+STD2(3)*X^2+STD2(4)*X+STD2(5)
; MAKE BASAL PLANE DATA
; FOR GR STANDARD

IF (CODE EQ 7) OR (CODE EQ 8) THEN BEGIN
    Y4=STD3(0)*X^5+STD3(1)*X^4+STD3(2)*X^3+STD3(3)*X^2+STD3(4)*X
; MAKE BASELINE FOR COMPRESSION
ENDIF

!GRID=2
!XTITLE='Temperature (C) '
!YTITLE='Delta L/Lo (microns/cm) '

```

```

!MTITLE='THERMAL EXPANSION  He atmosphere'
IF CODE EQ 2 THEN !XTITLE='TIME (minutes)'
  IF CODE EQ 3 THEN BEGIN
    !XTITLE='TIME (minutes)'
    !YTITLE='TEMPERATURE (C)'
  ENDIF
IF CODE EQ 4 THEN BEGIN
  !YTITLE='dS/dT (um/mm/deg.C)'
  !MTITLE='HIGH TEMPERATURE FLEXURE'
ENDIF
IF CODE EQ 9 THEN BEGIN
  !MTITLE='HIGH TEMPERATURE FLEXURE'
  !YTITLE='dS/dT (um/mm/C)'
ENDIF
IF CODE EQ 8 THEN BEGIN
  !MTITLE='HIGH TEMPERATURE COMPRESSION'
  !YTITLE='dL/dT (um/mm/C)'
ENDIF
IF CODE EQ 5 THEN BEGIN
  !YTITLE='dS/dt (um/cm/min.)'
  !XTITLE='Time (minutes)'
  !MTITLE='HIGH TEMPERATURE FLEXURE'
ENDIF
IF CODE EQ 6 THEN BEGIN
  !YTITLE='Deflection (um)'
  !XTITLE='Temperature (C)'
  !MTITLE='HIGH TEMPERATURE FLEXURE'
ENDIF
IF CODE EQ 7 THEN BEGIN
  !MTITLE='HIGH TEMPERATURE COMPRESSION'
  !YTITLE='Compressive Strain (10^-3)'
ENDIF

IF (CODE EQ 1) OR (CODE EQ 4) THEN BEGIN
  Y=(Y-Y1+Y2)/(C(1)+10) ; CORRECT DATA FOR DILATION SAMPLES
ENDIF

IF (CODE EQ 7) OR (CODE EQ 8) THEN BEGIN
  Y=(Y-Y4)/C(1) ; SUBTRACT COMPRESSION BASELINE
  ; AND MAKE INTO um/mm
ENDIF

IF (CODE EQ 6) OR (CODE EQ 9) THEN BEGIN
  Y=Y-PYROFLX ; SUBTRACT FLEXURE BASELINE
ENDIF

SET_VIEWPORT,.11,.80,.22,.9

IF Z GT 1 THEN BEGIN ; USE 'PLOT' ONLY IF 1ST TIME AROUND
  !LINETYPE=I-1
  IF (CODE EQ 1) OR (CODE EQ 6) OR (CODE EQ 7) THEN OPLLOT,X,SMOOTH(Y,NUMP)
  ; ELSE USE 'OPLLOT'
  IF CODE EQ 2 THEN OPLLOT,XT,SMOOTH(Y,NUMP) ; TIME:EXPANSION
  IF CODE EQ 3 THEN OPLLOT,XT,X
  IF (CODE EQ 4) OR (CODE EQ 8) OR (CODE EQ 9) THEN BEGIN
    Dy=DERIV(X,(SMOOTH(Y,NUMP)))
    Dy(0)=Dy(3)
    Dy(1)=Dy(0)
    OPLLOT,X,Dy
  ENDIF
ENDIF

```

```

ENDIF
IF CODE EQ 5 THEN BEGIN
  Dy=DERIV(XT, (SMOOTH(Y, NUMP)))
  Dy(0)=Dy(3)
  Dy(1)=Dy(0)
  OPLLOT, XT, Dy
ENDIF
ENDIF ELSE BEGIN

!PSYM=3 ; DO DOTS
VT100
!LINETYPE=0
PLOT, X, Y

IF (CODE EQ 1) OR (CODE EQ 6) OR (CODE EQ 7) THEN PLOT, X, Y
IF CODE EQ 2 THEN PLOT, XT, Y
IF CODE EQ 3 THEN PLOT, XT, X
IF (CODE EQ 4) OR (CODE EQ 8) OR (CODE EQ 9) THEN BEGIN
  Dy=DERIV(X, (SMOOTH(Y, NUMP)))
  Dy(0)=Dy(3) ; GENERAL DERIVATIVE CURVES
  Dy(1)=Dy(0)
  PLOT, X, Dy
ENDIF
IF CODE EQ 5 THEN BEGIN
  Dy=DERIV(XT, (SMOOTH(Y, NUMP)))
  Dy(0)=Dy(3)
  Dy(1)=Dy(0)
  PLOT, XT, Dy
ENDIF

!PSYM=0

IF PVAR NE 'Y' THEN BEGIN ; OPLLOT SMOOTHED CURVE
  SET XY
  !PSYM=0
  !LINETYPE=0
  IF (CODE EQ 1) OR (CODE EQ 6) OR (CODE EQ 7) THEN OPLLOT, X, SMOOTH(Y, NUMP)
  IF CODE EQ 2 THEN OPLLOT, XT, SMOOTH(Y, NUMP)
  IF CODE EQ 3 THEN OPLLOT, XT, X
  IF (CODE EQ 4) OR (CODE EQ 8) OR (CODE EQ 9) THEN BEGIN
    Dy=DERIV(X, (SMOOTH(Y, NUMP)))
    Dy(0)=Dy(3)
    Dy(1)=Dy(0)
    OPLLOT, X, Dy
  ENDIF
  IF CODE EQ 5 THEN BEGIN
    Dy=DERIV(XT, (SMOOTH(Y, NUMP)))
    Dy(0)=Dy(3)
    Dy(1)=Dy(0)
    OPLLOT, XT, Dy
  ENDIF
ENDIF

ENDIF

IF PVAR EQ 'Y' THEN BEGIN ; OPLLOT POLYNOMIAL CURVE IF
  COEFF=POLY_FIT(X, Y, ORD, GGG) ; PVAR=Y
  !PSYM=0
  OPLLOT, X, GGG
ENDIF

```

Z=2
ENDELSE

ENDFOR

```
!NOERAS=1
SET VIEWPORT,0,1,0,1
SET XY,0,1,0,1
ABCD=.82
XYOUTS,.85,.86,'Names: '
FOR LL=1,AB DO BEGIN
NNN=FINDGEN(AB+1)
!LINETYPE=NNN(LL-1)
OPLOT, [.82,.86], [ABCD-(LL-1)*.05,ABCD-(LL-1)*.05]
XYOUTS,.875,ABCD-(LL-1)*.05-.01,NAME(LL-1)
ENDFOR
SET XY
SET VIEWPORT
!NOERAS=0
```

```
SET VIEWPORT,0,1,0,1
SET XY,0,1,0,1
XYOUTS,.17,.1,'Name, Run Date: '
XYOUTS,.39,.1,A
XYOUTS,.17,.05,'Heating Rate (C/min.): '
XYOUTS,.455,.05,C(0)
XYOUTS,.7,.05,'Lo (cm): '
XYOUTS,.79,.05,C(1)
XYOUTS,.17,.075,'Sample ID: '
XYOUTS,.37,.075,B
```

```
SET XY
SET VIEWPORT,.11,.80,.22,.9
```

; *****

;PLOTting SECTION

; *****

PRINT, ' SAVE THIS ? [Y/N]'

YN=''

READ,YN

IF YN EQ 'Y' THEN BEGIN

; IF HARD COPY IS DESIRED

Z=1

for i=1,ab do begin

; do plotting...

OPENB,1,NAME(I-1)

A=STRARR(30,1)

B=STRARR(80,1)

C=fltarr(4)

D=''

E=DOUBLE(FLTARR(4,NUM(I-1)+1))

; MAKE DATA VECTOR DOUBLE PRECISION

READF,1,A,B,C,D,E

CLOSE,1

X=E(2,0:NUM(I-1))

; DEFINE NEW VARIABLES AND SET UP PLOT

```

Y=E(1,0:NUM(I-1))           ; MICRONS
XT=E(3,0:NUM(I-1))          ; TIME
PYROFLX=(-6.6E-3)*X

                                ; FOR FLEX SAMPLES

Y=Y-(Y(0)+Y(1)+Y(2))/3      ; SET ZERO OF CURVE

X=X/8
Y1=STD1(0)*X^7+STD1(1)*X^6+STD1(2)*X^5+STD1(3)*X^4+STD1(4)*X^3+STD1(5)*X^2+STD1(6)*X+STD1(7)
                                ; MAKE BASELINE DATA
X=X*8
Y2=STD2(0)*X^5+STD2(1)*X^4+STD2(2)*X^3+STD2(3)*X^2+STD2(4)*X+STD2(5)
                                ; MAKE BASAL PLANE DATA
                                ; FOR GR STANDARD

IF (CODE EQ 1) OR (CODE EQ 4) THEN BEGIN
  Y=(Y-Y1+Y2)/(C(1)+10)      ; CORRECT DATA FOR DILATION SAMPLES
ENDIF

IF (CODE EQ 7) OR (CODE EQ 8) THEN BEGIN
  Y=(Y-Y4)/C(1)              ; SUBTRACT COMPRESSION BASELINE
                                ; AND MAKE INTO  $\mu\text{m}/\text{mm}$ 
ENDIF

IF (CODE EQ 6) OR (CODE EQ 9) THEN BEGIN
  Y=Y-PYROFLX                 ; SUBTRACT FLEXURE BASELINE
ENDIF

!fancy = 2
set_plot,4

SET_VIEWPORT,.11,.80,.22,.9

IF Z GT 1 THEN BEGIN          ; USE 'PLOT' ONLY IF 1ST TIME AROUND
  !LINETYPE=I-1
  IF (CODE EQ 1) OR (CODE EQ 6) OR (CODE EQ 7) THEN OPLOT,X,SMOOTH(Y,NUMP)
                                ; ELSE USE 'OPLOT'
  IF CODE EQ 2 THEN OPLOT,XT,SMOOTH(Y,NUMP) ; TIME:EXPANSION
  IF CODE EQ 3 THEN OPLOT,XT,X
  IF (CODE EQ 4) OR (CODE EQ 8) OR (CODE EQ 9) THEN BEGIN
    Dy=DERIV(X,(SMOOTH(Y,NUMP)))
    Dy(0)=Dy(3)
    Dy(1)=Dy(0)
    OPLOT,X,Dy
  ENDIF
  IF CODE EQ 5 THEN BEGIN
    Dy=DERIV(XT,(SMOOTH(Y,NUMP)))
    Dy(0)=Dy(3)
    Dy(1)=Dy(0)
    OPLOT,XT,Dy
  ENDIF
ENDIF ELSE BEGIN

!PSYM=3                       ; DO DOTS
VT100
!LINETYPE=0
PLOT,X,Y

IF (CODE EQ 1) OR (CODE EQ 6) OR (CODE EQ 7) THEN PLOT,X,Y

```

```

IF CODE EQ 2 THEN PLOT,XT,Y
IF CODE EQ 3 THEN PLOT,XT,X
IF (CODE EQ 4) OR (CODE EQ 8) OR (CODE EQ 9) THEN BEGIN
    Dy=DERIV(X, (SMOOTH(Y,NUMP)))
    Dy(0)=Dy(3) ; GENERAL DERIVATIVE CURVES
    Dy(1)=Dy(0)
    PLOT,X,Dy
ENDIF
IF CODE EQ 5 THEN BEGIN
    Dy=DERIV(XT, (SMOOTH(Y,NUMP)))
    Dy(0)=Dy(3)
    Dy(1)=Dy(0)
    PLOT,XT,Dy
ENDIF

!PSYM=0

IF PVAR NE 'Y' THEN BEGIN ;OPLLOT SMOOTHED CURVE
    SET XY
    !PSYM=0
    !LINETYPE=0
    IF (CODE EQ 1) OR (CODE EQ 6) OR (CODE EQ 7) THEN OPLLOT,X,SMOOTH(Y,NUMP)
    IF CODE EQ 2 THEN OPLLOT,XT,SMOOTH(Y,NUMP)
    IF CODE EQ 3 THEN OPLLOT,XT,X
    IF (CODE EQ 4) OR (CODE EQ 8) OR (CODE EQ 9) THEN BEGIN
        Dy=DERIV(X, (SMOOTH(Y,NUMP)))
        Dy(0)=Dy(3)
        Dy(1)=Dy(0)
        OPLLOT,X,Dy
    ENDIF
    IF CODE EQ 5 THEN BEGIN
        Dy=DERIV(XT, (SMOOTH(Y,NUMP)))
        Dy(0)=Dy(3)
        Dy(1)=Dy(0)
        OPLLOT,XT,Dy
    ENDIF
ENDIF

XYOUTS, !CXMAX+0.843, !CYMAX+1.02, !STIME

IF PVAR EQ 'Y' THEN BEGIN ; OPLLOT POLYNOMIAL CURVE IF
    COEFF=POLY_FIT(X,Y,ORD,GGG) ; PVAR=Y
    !PSYM=0
    OPLLOT,X,GGG
ENDIF

Z=2
ENDELSE
ENDFOR
endif

IF CODE EQ 1 THEN BEGIN

IF Z EQ 2 THEN BEGIN

IF AB EQ 1 THEN BEGIN

PRINT, ' TO CALCULATE ALPHA, ENTER NUMBER OF REGIONS TO BE FITTED. '

```

```

PRINT, ' TO END, ENTER ZERO'
ANSWER=0
READ,ANSWER
if ANSWER GT 0 THEN BEGIN
  FOR I=1,ANSWER DO BEGIN
    PRINT, ' '
    PRINT, ' ENTER TEMP RANGE (LOWER,UPPER)'
    LOWER=5
    UPPER=5
    READ,LOWER,UPPER
    LOWER=MIN(WHERE(X GT LOWER))           ; GET SUBSCRIPTS OF TEMP RANGE
    UPPER=MAX(WHERE(X LT UPPER))
    XFIT=X(LOWER:UPPER)                   ; DEFINE NEW DATA VECTORS FOR
    YFIT=Y(LOWER:UPPER)                   ; ALPHA FIT
    COEFF=POLY FIT(XFIT,YFIT,1,LINE)      ; FIT LINE TO DATA
    !LINETYPE=8
    OPLOT,XFIT,LINE

    ALPHA=COEFF(1)*100                    ; MAKE ALPHA INTO MICRONS PER METER
    XYOUTS,X(UPPER),Y(UPPER),ALPHA
    SET_PLOT,0

  SET_VIEWPORT,.11,.80,.22,.9

    !FANCY=0
    OPLOT,XFIT,LINE
    XYOUTS,X(UPPER),Y(UPPER),ALPHA
    SET_PLOT,4

  SET_VIEWPORT,.11,.80,.22,.9

    !FANCY=3

  ENDFOR
ENDIF
ENDIF

ENDIF

ENDIF

IF YN EQ 'Y' THEN BEGIN

  !NOERAS=1
  SET_VIEWPORT,0,1,0,1
  SET_XY,0,1,0,1
  ABCD=.82
  XYOUTS,.85,.86,'Names:'
  FOR LL=1,AB DO BEGIN
    NNN=FINDGEN(AB+1)
    !LINETYPE=NNN(LL-1)
    OPLOT, [.80,.87], [ABCD-(LL-1)*.05,ABCD-(LL-1)*.05]
    XYOUTS,.875,ABCD-(LL-1)*.05-.01,NAME(LL-1)
  ENDFOR
  XYOUTS,.17,.1,'Name, Run Date: '
  XYOUTS,.31,.1,A
  XYOUTS,.17,.05,'Heating Rate (C/min.): '
  XYOUTS,.33,.05,C(0)
  XYOUTS,.8,.05,'Lo (cm): '

```

```
XYOUTS,.67,.05,C(1)
XYOUTS,.17,.075,'Sample ID: '
XYOUTS,.29,.075,B
```

```
'SET XY
SET VIEWPORT,.11,.80,.22,.9
!NOERAS=0
```

```
VT100
PRINT,' LASER PRINTING THE FILE NOW...'
WAIT,2
SET PLOT,0
VT100
SPAWN,'LASE_DOWN QMSFLOT.LIS'
ENDIF
```

```
SET_PLOT,0
```

```
end
```

TECHNOLOGY OPERATIONS

The Aerospace Corporation functions as an "architect-engineer" for national security programs, specializing in advanced military space systems. The Corporation's Technology Operations supports the effective and timely development and operation of national security systems through scientific research and the application of advanced technology. Vital to the success of the Corporation is the technical staff's wide-ranging expertise and its ability to stay abreast of new technological developments and program support issues associated with rapidly evolving space systems. Contributing capabilities are provided by these individual Technology Centers:

Electronics Technology Center: Microelectronics, solid-state device physics, VLSI reliability, compound semiconductors, radiation hardening, data storage technologies, infrared detector devices and testing; electro-optics, quantum electronics, solid-state lasers, optical propagation and communications; cw and pulsed chemical laser development, optical resonators, beam control, atmospheric propagation, and laser effects and countermeasures; atomic frequency standards, applied laser spectroscopy, laser chemistry, laser optoelectronics, phase conjugation and coherent imaging, solar cell physics, battery electrochemistry, battery testing and evaluation.

Mechanics and Materials Technology Center: Evaluation and characterization of new materials: metals, alloys, ceramics, polymers and their composites, and new forms of carbon; development and analysis of thin films and deposition techniques; nondestructive evaluation, component failure analysis and reliability; fracture mechanics and stress corrosion; development and evaluation of hardened components; analysis and evaluation of materials at cryogenic and elevated temperatures; launch vehicle and reentry fluid mechanics, heat transfer and flight dynamics; chemical and electric propulsion; spacecraft structural mechanics, spacecraft survivability and vulnerability assessment; contamination, thermal and structural control; high temperature thermomechanics, gas kinetics and radiation; lubrication and surface phenomena.

Space and Environment Technology Center: Magnetospheric, auroral and cosmic ray physics, wave-particle interactions, magnetospheric plasma waves; atmospheric and ionospheric physics, density and composition of the upper atmosphere, remote sensing using atmospheric radiation; solar physics, infrared astronomy, infrared signature analysis; effects of solar activity, magnetic storms and nuclear explosions on the earth's atmosphere, ionosphere and magnetosphere; effects of electromagnetic and particulate radiations on space systems; space instrumentation; propellant chemistry, chemical dynamics, environmental chemistry, trace detection; atmospheric chemical reactions, atmospheric optics, light scattering, state-specific chemical reactions and radiative signatures of missile plumes, and sensor out-of-field-of-view rejection.